Ocean Engineering 35 (2008) 1090–1101

Contents lists available at ScienceDirect

Ocean Engineering

journal homepage: www.elsevier.com/locate/oceaneng

Implementation and evaluation of alternative wave breaking formulas in a coastal spectral wave model

Jinhai Zheng [a,*], Hajime Mase [b], Zeki Demirbilek [c], Lihwa Lin [c]

[a] State Key Laboratory of Hydrology-Water Resources and Hydraulic Engineering, Hohai University, Nanjing, Jiangsu 210098, China
[b] Disaster Prevention Research Institute, Kyoto University, Gokasho, Uji, Kyoto 611-0011, Japan
[c] US Army Engineer Research and Development Center, Coastal and Hydraulics Laboratory, 3909 Halls Ferry Road, Vicksburg, MS 39180, USA

ARTICLE INFO

Article history:
Received 6 May 2007
Accepted 1 May 2008
Available online 10 May 2008

Keywords:
Numerical models
Random waves
Currents
Wave action
Breaking waves
Energy dissipation

ABSTRACT

This paper describes methods and results of research for incorporating four different parameterized wave breaking and dissipation formulas in a coastal wave prediction model. Two formulations assume the breaking energy dissipation to be limited by the Rayleigh distribution, whereas the other two represent the breaking wave energy by a bore model. These four formulations have been implemented in WABED, a directional spectral wave model based on the wave action balance equation with diffraction, reflection, and wave–current interaction capabilities. Four parameterized wave breaking formulations are evaluated in the present study using two high-quality laboratory data sets. The first data set is from a wave transformation experiment at an idealized inlet entrance, representing four incident irregular waves in a slack tide and two steady-state ebb current conditions. The second data set is from a laboratory study of wave propagation over a complex bathymetry with strong wave-induced currents. Numerical simulation results show that with a proper breaking formulation the wave model can reproduce laboratory data for waves propagating over idealized or complicated bathymetries with ambient currents. The extended Goda wave breaking formulation with a truncated Rayleigh distribution, and the Battjes and Janssen formulation with a bore model produced the best agreement between model and data.

1. Introduction

As waves approach the shore, their heights, lengths and directions are changed due to shoaling, refraction, diffraction, reflection and breaking as a consequence of the particular bathymetric and geometric features, as well as encounter with currents and structures present. Because reliable wave predictions in the coastal areas are crucial to engineering applications associated with shore protection, sediment management, harbor construction, navigation channel maintenance and maritime disaster reduction, numerical modeling of nearshore wave transformation has been a subject of considerable interest. In the past three decades, significant advances have occurred in the wave modeling. Many wave transformation models have been developed by using different type of linear and nonlinear wave theories for propagation of monochromatic or irregular waves over an arbitrary bathymetry. Because all wave models have certain advantages and limitations, their appropriateness in the coastal applications is largely dependent on type of physical processes at the project site.

Because waves are random in the real world setting, it is necessary to take into account their random nature in the wave transformation models. Mase and Kitano (2000), Nwogu and Demirbilek (2001), and Zubier et al. (2003) have classified random wave transformation models into two categories. The first category includes models based on the energy balance equation or wave action equation. Examples are TOMAWAC (Benoit et al., 1996), GHOST (Rivero et al., 1997), STWAVE (Smith et al., 1999), SWAN (Booij et al., 1999), and EBED (Mase, 2001). These frequency-domain models are suited to directional wave transformation over large areas of open oceans but have in recent years become increasingly popular for modeling neashore waves. The second category of wave models includes phase-resolving, refined time-domain models based on the conservation of mass and momentum equations. The Boussinesq family of wave models belongs to this class. These phase-resolving, time-domain models are generally more resources demanding, and appropriate for applications to relatively small coastal areas in shallow water to accurately represent wave profile, wave set-up, wave-induced current by solving mass and momentum equations (e.g. Peregrine, 1967; Madsen and Sorensen, 1992; Nwogu, 1993; Nwogu and Demirbilek, 2001).

* Corresponding author. Tel.: +86 25 83787706; fax: +86 25 83701905.
E-mail address: jhzheng@hhu.edu.cn (J. Zheng).

0029-8018/$ - see front matter © 2008 Published by Elsevier Ltd.
doi:10.1016/j.oceaneng.2008.05.001

Report Documentation Page

Form Approved
OMB No. 0704-0188

1. REPORT DATE	2. REPORT TYPE	3. DATES COVERED
2008		**00-00-2008 to 00-00-2008**

4. TITLE AND SUBTITLE	5a. CONTRACT NUMBER
Implementation and evaluation of alternative wave breaking formulas in a coastal spectral wave model	5b. GRANT NUMBER
	5c. PROGRAM ELEMENT NUMBER
6. AUTHOR(S)	5d. PROJECT NUMBER
	5e. TASK NUMBER
	5f. WORK UNIT NUMBER
7. PERFORMING ORGANIZATION NAME(S) AND ADDRESS(ES) **State Key Laboratory of Hydrology-Water Resources and Hydraulic Engineering,Hohai University,Nanjing, Jiangsu 210098, China, ,**	8. PERFORMING ORGANIZATION REPORT NUMBER
9. SPONSORING/MONITORING AGENCY NAME(S) AND ADDRESS(ES)	10. SPONSOR/MONITOR'S ACRONYM(S)
	11. SPONSOR/MONITOR'S REPORT NUMBER(S)

12. DISTRIBUTION/AVAILABILITY STATEMENT
Approved for public release; distribution unlimited

13. SUPPLEMENTARY NOTES

14. ABSTRACT

15. SUBJECT TERMS

16. SECURITY CLASSIFICATION OF:			17. LIMITATION OF ABSTRACT	18. NUMBER OF PAGES	19a. NAME OF RESPONSIBLE PERSON
a. REPORT	b. ABSTRACT	c. THIS PAGE			
unclassified	**unclassified**	**unclassified**	**Same as Report (SAR)**	**12**	

In some coastal areas such as tidal inlets and estuaries, where a great deal of human activity is located, the tidal currents can be strong and their effects on wave transformation cannot be neglected. Often waves are shortened and steepened by ebb currents, leading to considerable wave breaking outside and in the navigation channels. If currents are strong, wave blocking can happen, and considerable navigation hazard conditions can occur. For flood tides, waves are lengthened and their heights are reduced by current. In this case, larger non-breaking waves inside the channel may occur as compared to the ebb current case. In parts of the nearshore areas with a complicated bathymetry, strong wave-induced currents can create converging or diverging wave energy zones. The Doppler shift phenomenon affects wave refraction, reflection, and breaking that can significantly modify the overall redistribution of wave energy over the wave spectra frequencies and directions. Under such circumstances, the effects of ambient currents on nearshore wave transformations must be taken into account in the wave predictions for coastal projects.

One of important factors in modeling nearshore waves is the choice of wave breaking formulation. In the nearshore zone, once waves start to break, the turbulent dissipation of energy becomes the dominant dissipative mechanism, and breaking processes control the spatial variation of wave heights. In the absence of ambient currents, Zhao et al. (2001) and Zubier et al. (2003) have shown that different formulas for parameterization of wave breaking can yield large differences in wave height estimates in the surf zone. They demonstrated with a two-dimensional elliptic wave model and a spectral wave model that the formulation of Battjes and Janssen (1978) generally produced a good agreement between numerical estimates and data. In the presence of the ambient currents, many studies have been conducted to investigate effects of current on wave breaking (e.g., Yu, 1952; Iwagaki et al., 1980; Hedges et al., 1985; Lai et al., 1989; Sakai et al., 1988; Li and Dong, 1993; Briggs and Liu, 1993; Ris and Holthuijsen, 1996; Smith et al., 1998; Chawla and Kirby, 2002). However, no comprehensive evaluation of different wave breaking formulations in two-dimensional numerical models has been conducted for random wave transformation over a complicated bathymetry with ambient currents. A field evaluation of wave breaking parameterizations has been reported by Smith (2001). Lin and Demirbilek (2005) used a data set for irregular waves collected around an ideal tidal inlet in the laboratory as a benchmark to examine the performance of two spectral wave models. They found that both models considerably underestimated wave heights seaward of the inlet, suggesting that further investigation of wave breaking and wave–current interaction near inlets are necessary for improved spectral wave model estimates in coastal inlet projects.

The purpose of the present study was to evaluate four parameterized wave breaking formulations implemented in WABED (Mase and Kitano, 2000; Mase, 2001; Mase et al., 2005a, b; Lin et al., 2006, 2008) for coastal spectral wave transformation. This is accomplished by adding different dissipation formulas to WABED and evaluating estimate of wave dissipation with different wave breaking formulations. Model predictions are compared to data collected from two laboratory experiments. In the first experimental study, wave measurements were made to determine effects of wave shoaling, breaking and steady ebb currents around an idealized inlet (Smith et al., 1998). This study covered a wide range of wave and current parameters, and data obtained can be used in evaluation of wave dissipation formulations for current- and depth-induced wave breaking. The second experimental study investigated random wave transformation accompanied with wave breaking over a complicated bathymetry, where strong wave-induced nearshore currents were occurring.

2. Model description

2.1. Wave action balance equation with diffraction effect

A steady-state spectral model WABED (Mase et al., 2005a, b) is used to evaluate the parameterized wave breaking formulations. It is a 2-D phase-averaged model that neglects changes in the wave phase in calculating wave and other nearshore processes from the wave energy density. Both wave diffraction and reflection are included in approximate ways. To take the effect of ambient currents into account, the wave action density is used in WABED rather than the wave energy density since the wave action density is conserved whereas the wave energy density is not if waves travel with ambient currents (Bretherton and Garrett, 1968). The Doppler shift is considered in the wave dispersion equation implemented in WABED to develop a practice-oriented random wave model for coastal engineering studies at inlets, navigation projects, and wave–structure interactions (Lin et al., 2006, 2008). In these applications, wave breaking, dissipation, reflection, diffraction, and wave–current interaction are always important processes, and accurate representation of these processes is necessary for reliable estimate of waves in engineering design, maintenance, and operations. This paper investigates effects of parameterized wave breaking and dissipation on wave transformation in inlets and navigation channels. The frequency-dependent variation of wave action density resulting from wave–wave interactions is not considered in the present study, and will be addressed in a companion future paper.

The governing wave action balance equation with the wave diffraction effect as implemented in WABED model (Mase, 2001) is

$$\frac{\partial(C_x N)}{\partial x}+\frac{\partial(C_y N)}{\partial y}+\frac{\partial(C_\theta N)}{\partial \theta} = \frac{\kappa}{2\sigma}\left[(CC_g\cos^2\theta N_y)_y-\frac{1}{2}CC_g\cos^2\theta N_{yy}\right]-\varepsilon_b N \quad (1)$$

where N is the wave action density, defined as wave energy density divided by the angular frequency σ relative to a current (Doppler shift). The horizontal coordinates are (x, y), and θ is the wave direction measured counterclockwise from the x-axis. The first term in the right-hand side of Eq. (1) represents wave diffraction as formulated from the parabolic wave approximation assumption. A default value of $\kappa = 2.5$ is used for the diffraction intensity parameter in the present study. As suggested by Mase (2001), the appropriate values of κ should be estimated from laboratory and field data, and in the absence of data, the recommended value is 2.5. In Eq. (1), C and C_g are the wave celerity and group velocity, respectively, and ε_b is a parameterized wave breaking function for wave energy dissipation. The characteristic wave velocities with respect to x, y and θ coordinates are accordingly C_x, C_y, and C_θ, defined as

$$C_x = C_g\cos\theta + U \quad (2)$$

$$C_y = C_g\sin\theta + V \quad (3)$$

$$C_\theta = \frac{\sigma}{\sinh 2kh}\left(\sin\theta\frac{\partial h}{\partial x}-\cos\theta\frac{\partial h}{\partial y}\right)+\cos\theta\sin\theta\frac{\partial U}{\partial x} -\cos^2\theta\frac{\partial U}{\partial y}+\sin^2\theta\frac{\partial V}{\partial x}-\sin\theta\cos\theta\frac{\partial V}{\partial y} \quad (4)$$

where U and V are current velocity components in the x and y directions, respectively, and k is the wave number. The relationships between the relative angular frequency σ, absolute angular frequency ω, wave number vector $\mathbf{k}$, current velocity vector $\mathbf{U}$, and

the water depth h are

$$\sigma^2 = g|\mathbf{k}| \tanh |\mathbf{k}|h \tag{5}$$

$$\sigma = \omega - \mathbf{k}\cdot\mathbf{U} \tag{6}$$

The wave action balance equation with diffraction (Eq. (1)) is solved by a forward-marching first-order upwind finite-difference method. For given values at the offshore boundary, wave spectra and statistical quantities are calculated in the wave propagation direction at each column in a rectangular grid before moving forward to the next. WABED can optionally perform the backward marching for seaward reflection after completing the forward-marching calculations.

In the treatment of the dispersion relation with the Doppler shift, waves with large wave numbers were not considered in the original WABED (Mase et al., 2005a). However, the exclusion of large wave numbers (k) can in some cases lead to errors. In the present version, we use a quadratic solution for wave dispersion parameter $kh > 3\pi$, and set $\tanh kh = 1$ for large kh, and combine Eqs. (5) and (6) into one quadratic equation in terms of wave number as

$$k^2(U\cos\theta + V\sin\theta)^2 - [2(U\cos\theta + V\sin\theta)\omega + g]k + \omega^2 = 0 \tag{7}$$

The solution for the wave number in Eq. (7) is the smaller real root in order for the wave group velocity to be greater than the ambient current. For $kh < 3\pi$, the solution is obtained through an iterative scheme. If no solution exists for the dispersion relationship indicating a wave blocking condition, the wave action density is set to zero for the corresponding frequency and direction bin.

2.2. Parameterization of wave breaking energy dissipation

In Eq. (1), the parameterized function ε_b describes the mean energy dissipation rate per unit horizontal area due to wave breaking. The importance of this function is examined for four wave breaking formulas: (1) extended Miche formula, (2) extended Goda formula, (3) Chawla and Kirby formula, and (4) Battjes and Janssen formula. These formulas are divided into two generic categories. The first category describes the wave breaking energy dissipation with various breaker criteria and by truncating the tail of the Rayleigh distribution. The second category describes the integral (bulk) wave energy dissipation over the spectrum with a bore-type model. For additional information, see Zhao et al. (2001) and Zubier et al. (2003). A summary description of the parameterized wave breaking formulas is presented next.

2.2.1. Extended Miche's formula

Following Takayama et al. (1991), Mase et al. (2005a) formulated the wave energy dissipation rate ε_b using the extended Miche's breaking criteria:

$$\varepsilon_b = \left\{1 - \frac{1 - \left[1 + \frac{\pi}{4}\left(1.6\frac{H_{bo}}{H_{1/3}}\right)^2\right]\exp\left[-\frac{\pi}{4}\left(1.6\frac{H_{bo}}{H_{1/3}}\right)^2\right]}{1 - \left[1 + \frac{\pi}{4}\left(1.6\frac{H_{bi}}{H_{1/3}}\right)^2\right]\exp\left[-\frac{\pi}{4}\left(1.6\frac{H_{bi}}{H_{1/3}}\right)^2\right]}\right\} \times \frac{C}{dl} \tag{8}$$

where H_{bi} and H_{bo} are breaking wave heights at the seaside and landside of a cell, $H_{1/3}$ is the significant wave height, and dl is the grid size. Eq. (8) is valid if $H_{bi} > H_{bo}$ and $\varepsilon_b = 0$ otherwise. The extended Miche's formula reduces to a steepness limit in deep water and a depth limit in shallow water. Iwagaki et al. (1980) verified that the Miche's breaker criterion (1944) can be applied to a wide range of experimental data over a sloping beach with currents if the wavelength is calculated with current included in the wave dispersion relation. Battjes (1972) extended the Miche's criterion for variable depth as

$$\frac{H_b}{L_b} = 0.14\tanh\left(\frac{\gamma_b}{0.88}\frac{2\pi h}{L_b}\right) \tag{9}$$

where L_b is the wavelength at the breaking point with currents considered, and γ_b is an adjustable coefficient that varies with beach slope. In application to irregular waves, a constant value of $\gamma_b = 0.8$ is frequently adopted for a wide range of beach slopes and mean wave steepnesses (Battjes and Janssen, 1978; Zhao et al., 2001; Zubier et al., 2003). In WABED, a functional form as suggested by Ostendorf and Madsen (1979) is adapted

$$\gamma_b = \begin{cases} 0.8 + 5\tan\beta & \tan\beta < 0.1 \\ 1.3 & \tan\beta \geqslant 0.1 \end{cases} \tag{10}$$

where β denotes the local bottom slope angle.

The change in breaker height with respect to the cell length dl is expressed as

$$dH_b/dl = \begin{cases} -0.14\tan\beta\frac{\gamma_b}{0.88}2\pi\cosh^{-2}\left(\frac{\gamma_b}{0.88}\frac{2\pi h}{L_b}\right) & \tan\beta \geqslant 0 \\ 0 & \tan\beta < 0 \end{cases} \tag{11}$$

The breaking heights at each side of a cell in the computational grid are

$$H_{bi} = H_b - \frac{1}{2}dH_b \tag{12}$$

$$H_{bo} = H_b + \frac{1}{2}dH_b \tag{13}$$

2.2.2. Extended Goda's formula

Based on the laboratory data, Goda (1970) proposed a breaker criterion by taking into account the bottom slope and deep water wave steepness. In the presence of opposing currents, Sakai et al. (1988) introduced a proportional coefficient to account for the combined effects of unit width discharge, bottom slope, incident wave length, and local water depth. With this modification, the breaking wave height becomes

$$H_b = \begin{cases} 0.17L_0\left\{1 - \exp\left[-1.5\frac{\pi h}{L_0}(1 + 15\tan^{4/3}\beta)\right]\right\}c(\varepsilon_d) & \tan\beta \geqslant 0 \\ 0.17L_0\left\{1 - \exp\left[-1.5\frac{\pi h}{L_0}\right]\right\} & \tan\beta < 0 \end{cases} \tag{14}$$

where

$$c(\varepsilon_d) = \begin{cases} 0.506 & \varepsilon_d \geqslant 0.0024 \\ 1.13 - 260\varepsilon_d & 0.0024 > \varepsilon_d \geqslant 0.0005 \\ 1.0 & \varepsilon_d < 0.0005 \end{cases} \tag{15}$$

and

$$\varepsilon_d = \frac{q}{g^2T^3}(\tan^{1/4}\beta)\Big/(h/L_0) \tag{16}$$

where L_0 is the wavelength in deep water, q the unit width discharge, g the gravitational acceleration, and T the significant wave period for random waves.

The change in breaker height with respect to the cell is defined as

$$dH_b/dl = \begin{cases} -0.225\pi \tan\beta(1+15\tan^{4/3}\beta)c(\varepsilon_d) \times \exp\left[-1.5\frac{\pi h}{L_0}(1+15\tan^{4/3}\beta)\right] & \tan\beta \geqslant 0 \\ 0 & \tan\beta < 0 \end{cases} \quad (17)$$

The energy dissipation rate ε_b is calculated by combining Eqs. (8), (12)–(14) and (17).

2.2.3. Chawla and Kirby's formula

Thornton and Guza (1983) parameterized the wave breaking energy dissipation using the Rayleigh distribution and an empirical weighting function in a bore-type model. However, because their formula is independent on the local water depth, it cannot be used to model current-limited wave breaking. Using a similar approach, Chawla and Kirby (2002) proposed the following expression for bulk energy dissipation with the ambient current:

$$\langle D\rangle = \frac{3\lambda\rho}{32\sqrt{\pi}}\sqrt{\frac{(g\bar{k})^3}{\tanh\bar{k}h}}\left(\frac{\bar{k}}{\gamma\tanh\bar{k}h}\right)^2 \times H_{rms}^5\left[1-\left\{1+\left(\frac{\bar{k}H_{rms}}{\gamma\tanh\bar{k}h}\right)^2\right\}^{-5/2}\right] \quad (18)$$

where $\langle D\rangle$ is the bulk energy dissipation by all breaking waves, $\bar{k}$ is the wave number corresponding to the mean angular frequency $\bar{\sigma}$, H_{rms} is the root-mean-square wave height, and scaling parameters λ and γ are set to 0.4 and 0.6, respectively.

The wave breaking energy dissipation coefficient ε_b in Eq. (1) is calculated as

$$\varepsilon_b = \frac{\langle D\rangle}{(\rho g H_{rms}^2/8)\bar{\sigma}} \quad (19)$$

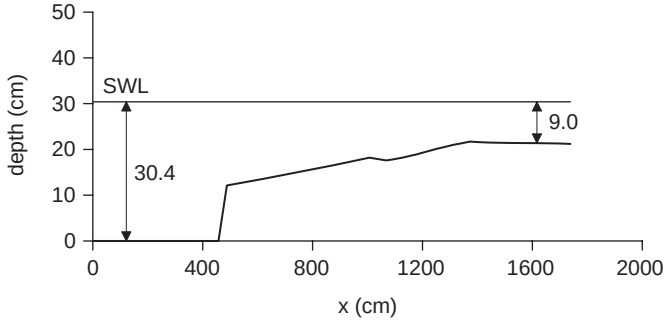

Fig. 1. Cross section of beach along the inlet channel centerline transect.

2.2.4. Battjes and Janssen's formula

Battjes and Janssen (1978) developed the following formula for the prediction of energy dissipation in random waves breaking on a beach:

$$\langle D\rangle = \frac{\alpha\rho g}{4}Q_b\bar{f}H_b^2 \quad (20)$$

where α is a constant of order one, $\bar{f}(=\bar{\sigma}/2\pi)$ is the mean relative frequency, and Q_b is the fraction of broken waves greater than the breaker height H_b in the Rayleigh distribution and as determined from the following equation:

$$\frac{1-Q_b}{\ln Q_b} = -\left(\frac{H_{rms}}{H_b}\right)^2 \quad (21)$$

In SWAN version 40.11 (Booij et al., 1999), a constant breaker parameter of $\gamma_b = 0.73$ was used in Eq. (9) to determine the breaking wave height H_b at the local water depth. Chen et al. (2005) also adopted this breaking criterion in their finite element coastal harbor wave model based on the extended mild slope equation with wave–current interaction. Eqs. (20) and (21) are used with Eq. (19) to calculate ε_b.

3. Numerical results and discussion

3.1. Wave shoaling and breaking around an idealized inlet

Smith et al. (1998) conducted a laboratory study to investigate the wave–current interaction and wave breaking in the presence of a steady ebb current at an idealized entrance. The physical model was built at an undistorted model-prototype scale of 1:50. The shore-parallel depth contours were determined by an equilibrium profile equation of Dean (1977) using a coefficient of 0.24. The sloping bathymetry in this model extended to 18.2 cm

Table 1
Incident wave parameters and current conditions for idealized inlet case

	H_{m0} (cm)	f_p (Hz)	U_{ave} (cm/s)	Notes
Case 1	5.77	0.78	11.5	Run 5 in the Technical Report CHL-98-31
Case 2	3.92	1.45	11.1	Run 8 in the Technical Report CHL-98-31
Case 3	5.97	0.78	21.9	Run 9 in the Technical Report CHL-98-31
Case 4	5.51	1.37	21.9	Run 11 in the Technical Report CHL-98-31

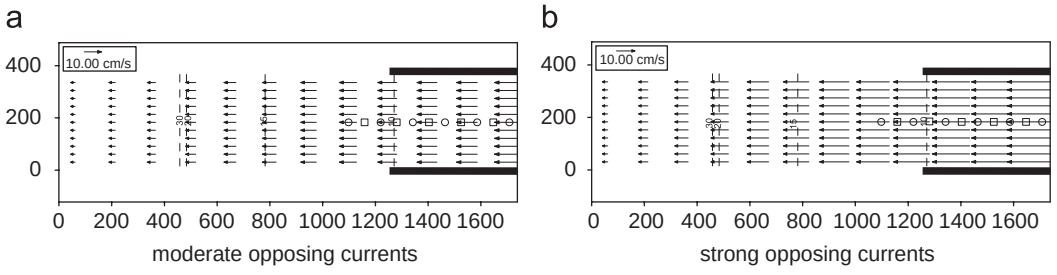

Fig. 2. Input current fields for idealized inlet case: (a) moderate opposing currents and (b) strong opposing currents.

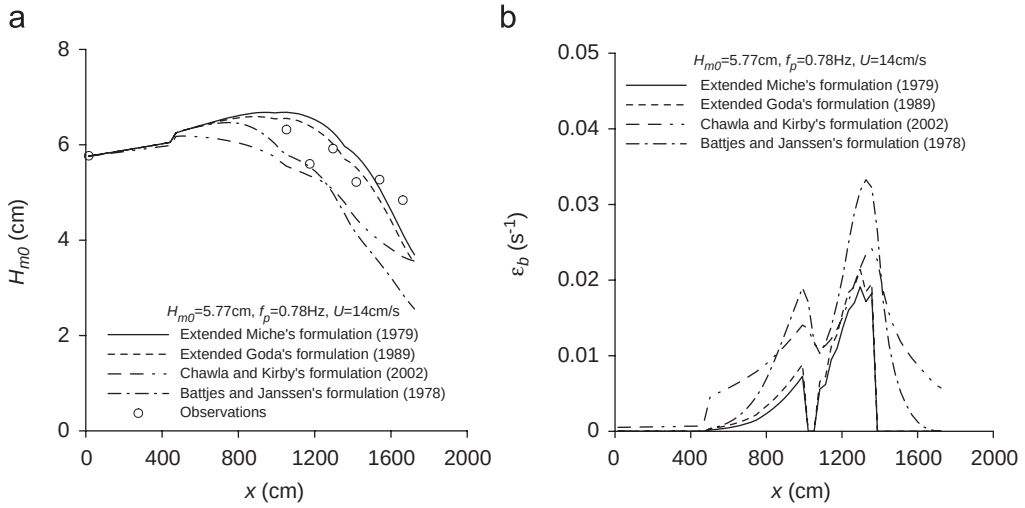

Fig. 3. Model results of wave height and energy dissipation along central transect for small peak frequency waves with moderate opposing currents: (a) wave height and (b) energy dissipation coefficient.

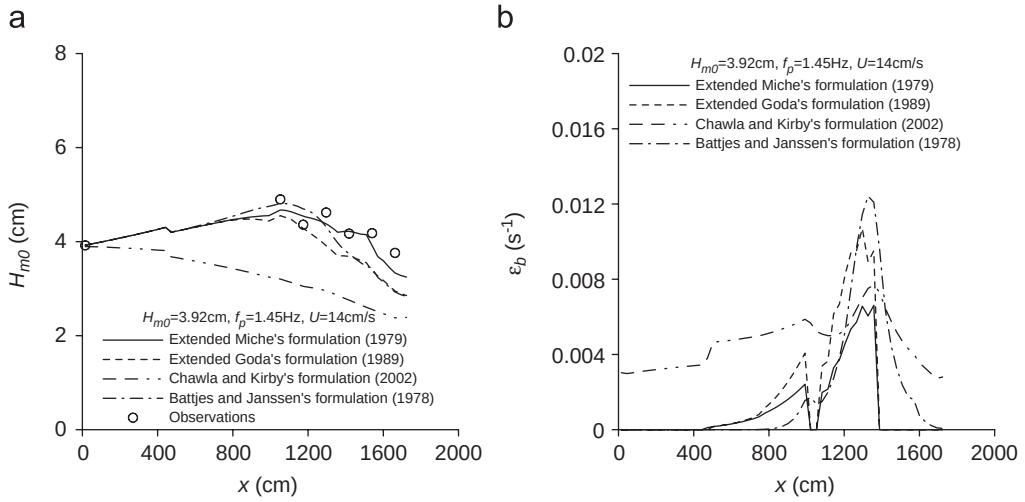

Fig. 4. Model results of wave height and energy dissipation along central transect for large peak frequency waves with moderate opposing currents: (a) wave height and (b) energy dissipation coefficient.

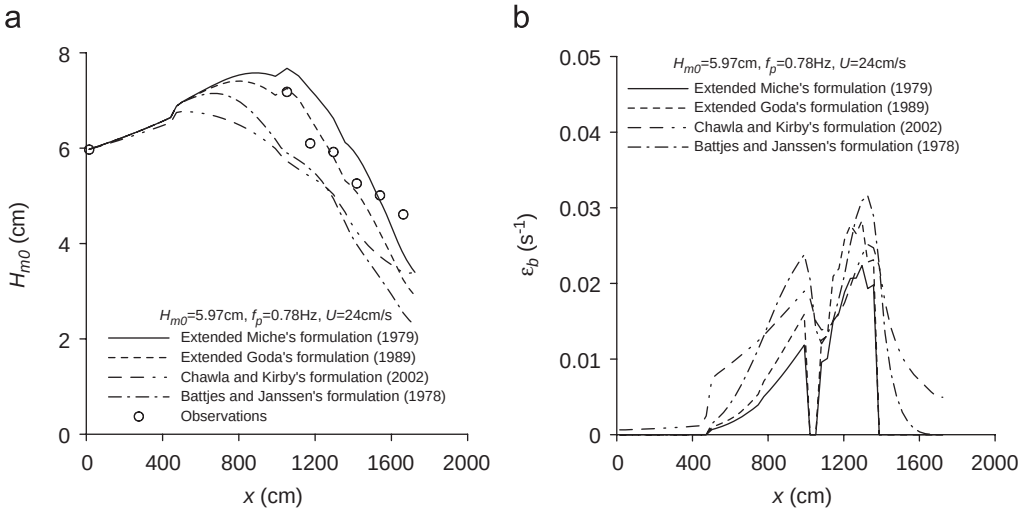

Fig. 5. Model results of wave height and energy dissipation along central transect for small peak frequency waves with strong opposing currents: (a) wave height and (b) energy dissipation coefficient.

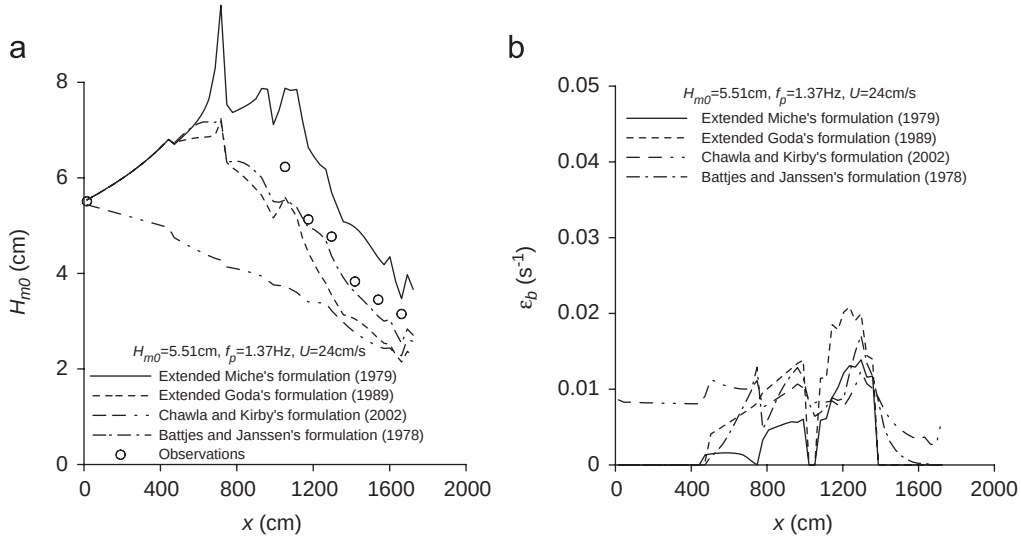

Fig. 6. Model results of wave height and energy dissipation along central transect for large peak frequency waves with strong opposing currents: (a) wave height and (b) energy dissipation coefficient.

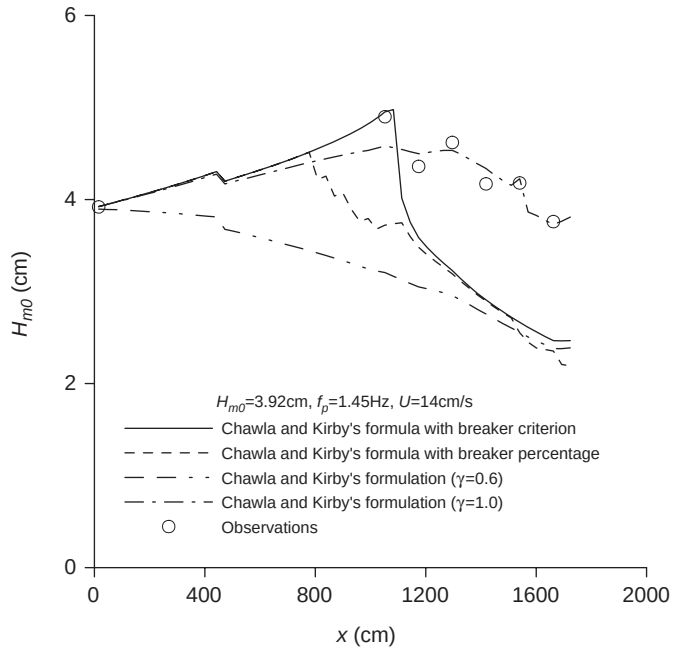

Fig. 7. Model to data comparisons using Chawla and Kirby's formulation and its modifications.

Table 2
Statistical mean errors and correlation coefficients for idealized inlet case

	MAERH (%)	Correlation coefficient
Extended Miche's formulation	18.9	0.88
Extended Goda's formulation	13.1	0.95
Chawla and Kirby's formulation ($\gamma = 0.6$)	25.5	0.79
Chawla and Kirby's formulation ($\gamma = 1.0$)	15.8	0.91
Chawla and Kirby 's formulation ($\gamma = 0.6$ add breaker criterion)	21.3	0.85
Chawla and Kirby's formulation ($\gamma = 0.6$ add breaker percentage)	22.7	0.84
Battjes and Janssen's formulation	14.5	0.93

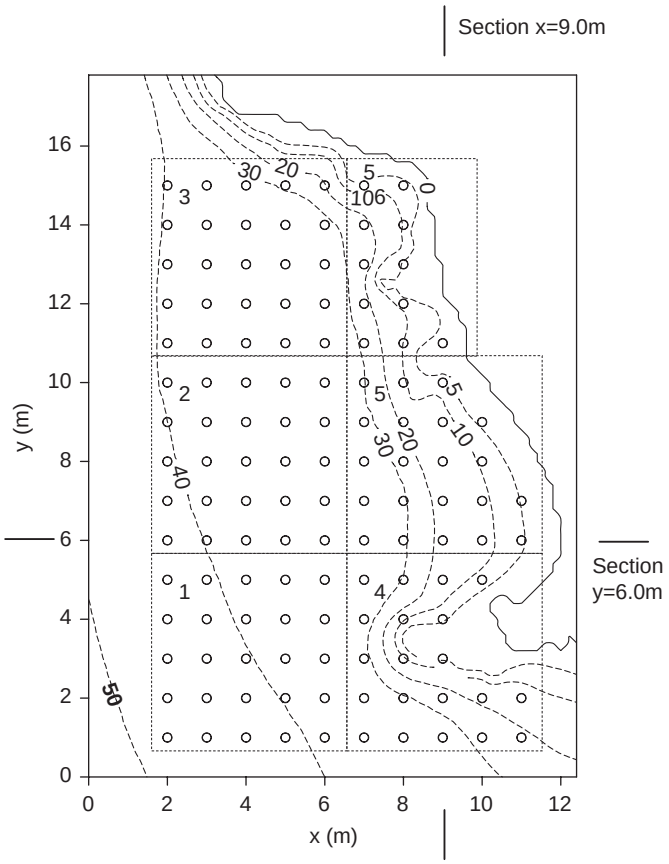

Fig. 8. Bathymetry and locations of wave gauges and currentmeters (circles)—depth contours shown as dash lines and labeled in centimeters.

mean low water depth, and was linearly transitioned to the basin floor at a depth of 30.4 cm. Two parallel jetties extending 550 cm offshore were spaced 366 cm apart, and built to create an entrance channel in which depths varied from 12.8 to 9.0 cm. The inlet throat region converged to a depth of 15.2 cm relative to a mean low water datum. Incident waves and current conditions were widely varied in 12 runs. Runs 1–4 were without a tidal current,

and Runs 5–8 had a moderate steady-state ebb current of approximately 11 cm/s at the inlet entrance. A strong steady-state ebb current of approximately 22 cm/s at the entrance was present in the Runs 9–12.

Wave and horizontal velocity data were collected with electrical capacitance gauges and acoustic doppler velocimeters (ADVs), respectively. The calibration error for wave height data was 1 mm, and the accuracy of velocity data was within 0.5% of the measured current. These laboratory data were compared to the wave model results to evaluate wave energy dissipation formulations for combined depth- and current-induced wave breaking. Because the data were collected only at handful locations, the performance of different breaking formulations in WABED was evaluated by simple statistics like normalized bias and root-mean-square error.

In the present study, the wave modeling of interest is at the inlet channel, where wave height, current velocity, and water depth were measured in the physical model. The computational grid covers a rectangular domain with 57 cells in the cross-shore direction and 12 cells in the long-shore direction. Computational cell sizes are $30.5 \times 30.5\,\text{cm}^2$ at the physical model scale and $15.3 \times 15.3\,\text{m}^2$ in the prototype. Wave gauges were deployed offshore in front of the wave generator, in the outside region of the inlet, and inside the inlet area between two parallel jetties. A TMA uni-directional wave spectrum with $\gamma = 3.3$ and 10 frequency bins was used to generate incident waves at the seaward boundary.

Table 3
Model test conditions for complicated bathymetric coast case

Return period (year)	1	5	10	20	100
Significant wave height (cm)	1.86	5.14	5.75	6.26	7.26
Significant wave period (s)	0.68	1.00	1.06	1.11	1.21

The water depths are linearly interpolated from the isobathic data, and depths between the two jetties are modified by still-water depths at gauges. The cross section of the beach along the inlet channel centerline transect is shown in Fig. 1. Current velocities were measured at spatially fixed locations. Because the detailed two-dimensional current field data were not available, the current velocity input in the numerical simulations was determined by a linear interpolation of data. Even though waves can modify the current field, the modification of the current by waves was beyond the scope of this paper and therefore it was not considered in the numerical model simulations. Fig. 2 shows an example of the interpolated current field for Run 5 and Run 11, where the circle and the square points denote positions of wave gauge and ADV, respectively. Numerical simulations were conducted at the prototype 1:50 scale. Table 1 presents incident wave parameters and ebb current conditions, where U_{ave} is the averaged velocity in the entrance channel.

Fig. 3 shows the example of numerical results for Run 5 with small peak frequency and moderate ebb currents. The wave height estimates obtained with the extended Miche's, extended Goda's, and Battjes and Janssen's formulas agree well with the experimental data. In this example, Chawla and Kirby's formula underpredicted the wave height because the calculated dissipation coefficients were relatively high as shown in Fig. 3(b).

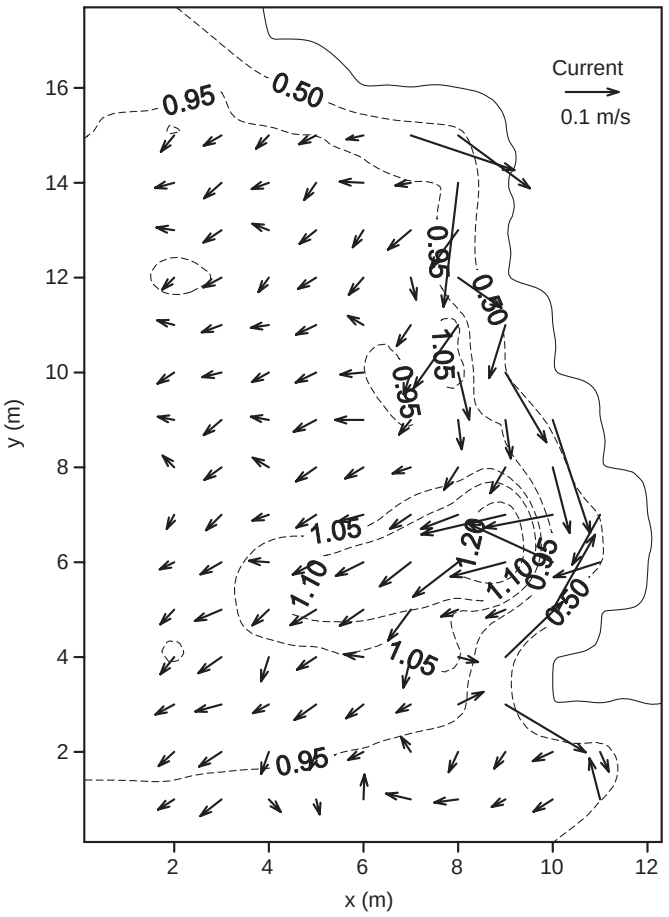

Fig. 9. Experimental results of significant wave heights (normalized by incident one) and wave-induced currents for uni-directional waves.

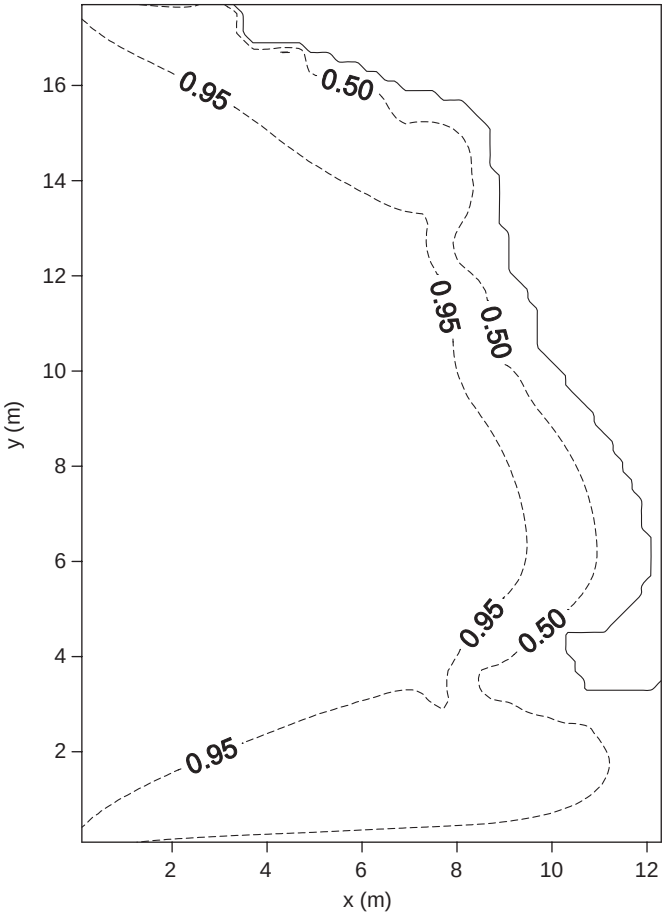

Fig. 10. Calculated wave field for uni-directional waves without currents (using Battjes and Janssen's formulation).

Fig. 4 shows the example of numerical results for Run 8 for a large peak frequency wave with a moderate opposing current. The results using the extended Miche's formula, extended Goda's formula, and Battjes and Janssen's formula agree well with data. On the other hand, Chawla and Kirby's formula substantially underpredicted the wave height because the wave breaking calculated by this formula generally occurs further offshore, producing larger wave dissipation as shown in Fig. 4(b).

Fig. 5 shows the example of numerical results for Run 9 for a small peak frequency wave and strong opposing currents. The trend in model predicted wave heights is similar to that for a small peak frequency wave with moderate opposing currents. The wave height estimates from the extended Goda's formula agree well with data. The calculated wave heights using the extended Miche's formula overestimate the wave height, owing to the relative smaller wave breaking energy dissipation as shown in Fig. 5(b). The estimates using the extended Goda's formula agree well with data. The formulas of Chawla and Kirby and Battjes and Janssen underpredicted the wave height.

Fig. 6 shows the example of numerical results for Run 11 for a large peak wave frequency and strong opposing currents. Calculated results show that the extended Miche's formula overpredicted the wave height while predictions by the extended Goda's and the Battjes and Janssen's formulas agreed better with data. The Chawla and Kirby's formula again underestimated the wave height.

The underprediction of wave height using Chawla and Kirby's formula is attributed to two factors. First, the calculated wave energy dissipation occurs offshore in relatively deep water because there is no limiting condition in this formula. Second, an excessive amount of wave energy dissipation occurs because of unknown value of γ arbitrarily chosen for an application that could be inappropriate. Consequently, it was necessary to modify Chawla and Kirby's formula to impose a limiting condition on wave breaking using Eqs. (9) and (10). This modification has been denoted in Fig. 7 as Chawla and Kirby's formula with the breaker criterion. A second alternative to modify the Chawla and Kirby's formula was to add a fraction of the breaking waves as defined in Eq. (21). This modification is denoted in Fig. 7 as Chawla and Kirby's formula with a breaker percentage. A third alternative was to use $\gamma = 1.0$ in Eq. (18). Results of wave heights calculated from these modifications are shown in Fig. 7. By imposing the limit condition with Miche's breaker criterion (the first modification) gave rise to a much stronger wave convergence (concentration of waves) in the intermediate water depth. The application of a limit condition to eliminate excess dissipation if waves were not breaking (the second modification) did not substantially improve model predictions as compared to measurements. For the large peak frequency wave and moderate opposing current, using $\gamma = 1.0$ (the third modification) in Eq. (18) produced only slightly better wave height estimates for all runs.

Two statistical parameters are applied to evaluate the overall performance of four different parameterized energy dissipation formulas in WABED (Table 2). The first statistics is the mean value of absolute relative error for the normalized significant wave height, defined as

$$\mathrm{MAERH} = \frac{1}{M}\sum_{i=1}^{M} \frac{\left|\left[\frac{H_{1/3}}{(H_{1/3})_0}\right]_{ci} - \left[\frac{H_{1/3}}{(H_{1/3})_0}\right]_{\mathrm{mi}}\right|}{\left[\frac{H_{1/3}}{(H_{1/3})_0}\right]_{\mathrm{mi}}} \times 100\% \qquad (22)$$

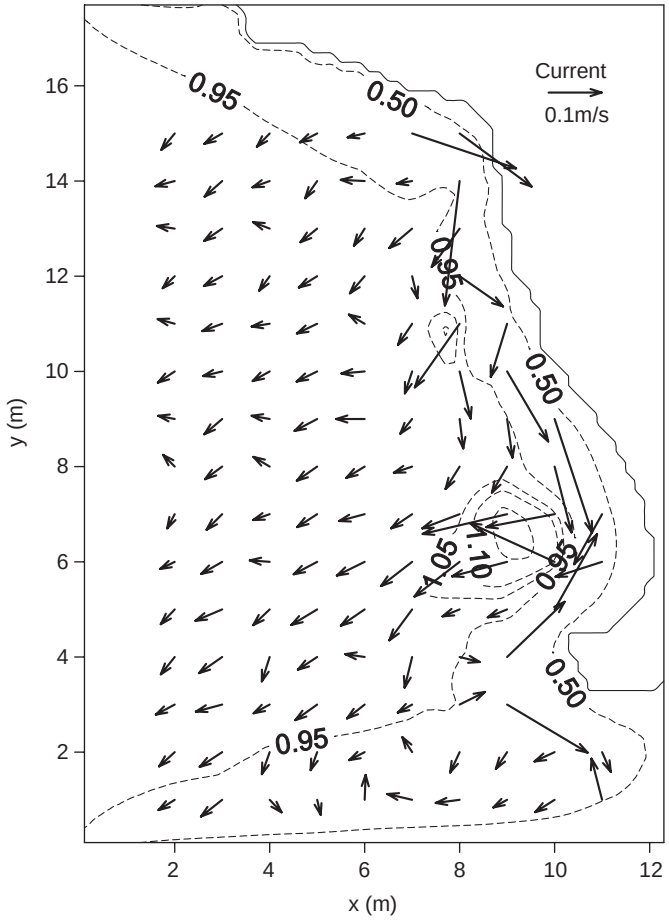

Fig. 11. Calculated wave field for uni-directional waves with currents (using extended Miche's formulation).

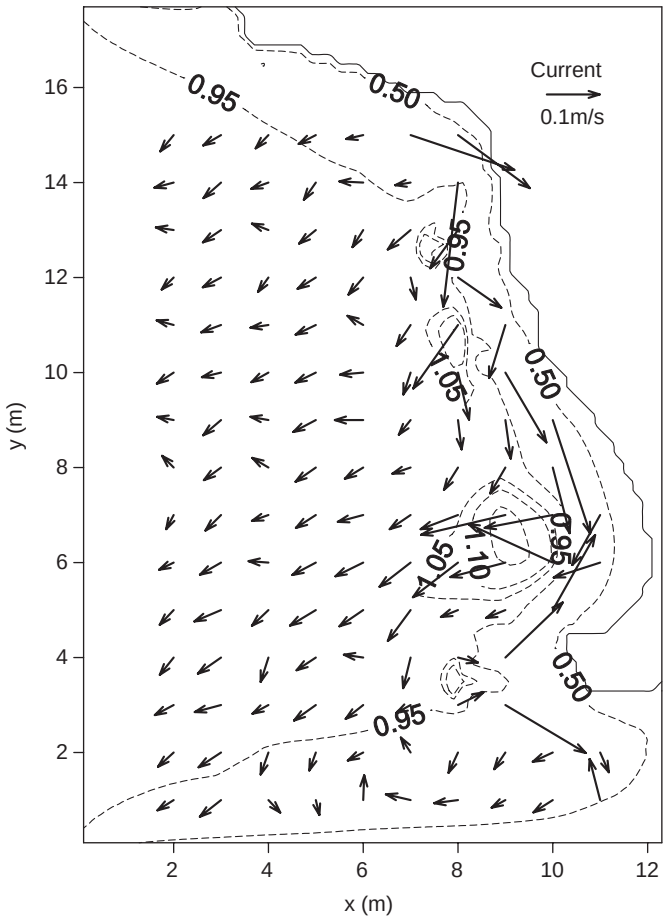

Fig. 12. Calculated wave field for uni-directional waves with currents (using extended Goda's formulation).

where $M = 60$ (total numbers of wave height data available in each experiment condition), and subscripts c and m denote the calculated and measured normalized significant wave height, respectively. A small value of MAERH indicates a good agreement between calculated wave model predictions and the experimental data. A value of zero implies a perfect match between computations and measurements. The second statistics used here is the correlation coefficient (equivalent to the normalized root-mean-square error) between calculated and measured normalized wave heights (Mase et al., 2005b).

Based on comparisons of calculated and measured wave heights in the idealized inlet experiment study (Figs. 3–7 and Table 2), the extended Goda's and the Battjes and Janssen's breaking formulas performed best for all wave conditions investigated herein. The extended Miche's formula performed well for small frequency waves or moderate currents, but it overpredicted wave heights for large peak frequency waves with strong opposing currents. The Chawla and Kirby's formula produced the largest wave dissipation and therefore underpredicted wave height in all simulations. For large peak frequency waves, this formula calculated excessive wave dissipation in the offshore region for non-breaking waves.

3.2. *Wave transformation over complicated bathymetry with strong nearshore currents*

Laboratory experiments were conducted at the Research and Development Department of the Kansai Electric Power Co. Inc., Japan to study the wave transformation over a complicated bathymetry near a power plant. Fig. 8 shows the beach built in the physical model in a wave basin of 20-m wide and 38-m long, with the water depth contours shown are in units of centimeter. The model-to-prototype Froude scale in these experiments was 1:125. Both uni-directional and multi-directional waves were generated by the wavemaker using the Bretscheider–Mitsuyasu type of wave spectrum (Mitsuyasu, 1970). The wave directional spreading function with a value of $S_{max} = 25$ was used for the multi-directional random waves. The wavemaker had 60 wave paddles, and each paddle was 30 cm wide. Table 3 shows wave conditions tested in the physical model.

Waves and currents were measured at 127 locations in six regions with electrical capacitance wave gauges and electromagnetic current meters shown as the small circles in Fig. 8. The current velocities were measured in the middle of the local water depth. The calibration error for wave height data is within 0.1 cm and the accuracy of velocity speed is within 1% of the measured current magnitude. Both wave and current data were collected for 400 s after wave paddles started to move, and the first 60 s data were discarded in the analysis.

For the case of 100-year's return period wave, that is, the incident waves at model scale having a significant wave height and period of 7.3 cm and 1.21 s, respectively, measurements indicated strong wave-induced nearshore currents developing, and the maximum measured current speed was up to 25 cm/s for uni-directional waves. These strong currents caused waves focusing in the vicinity of the concave coasts as shown in Fig. 9.

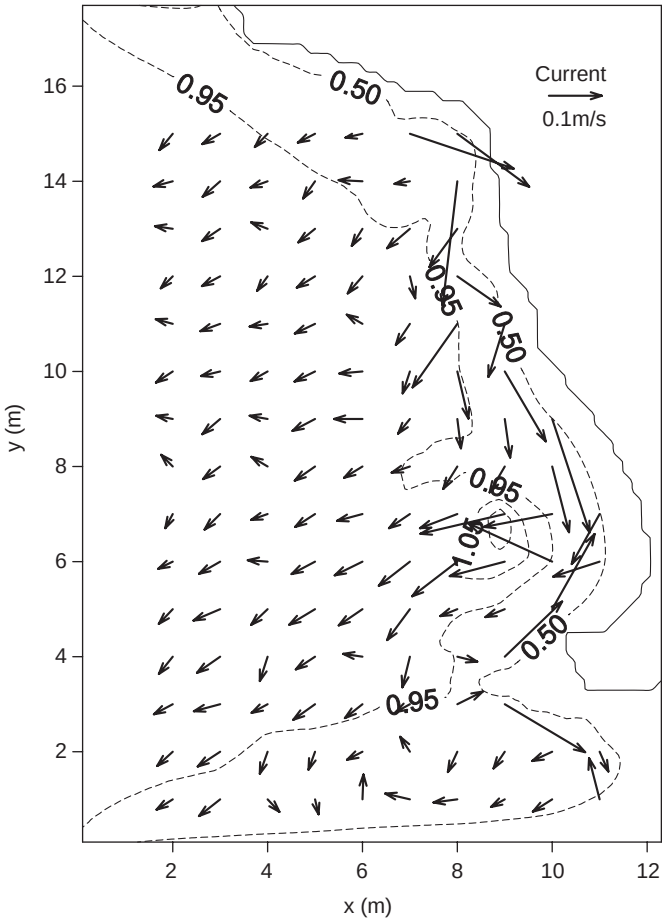

Fig. 13. Calculated wave field for uni-directional waves with currents (using Chawla and Kirby's formulation).

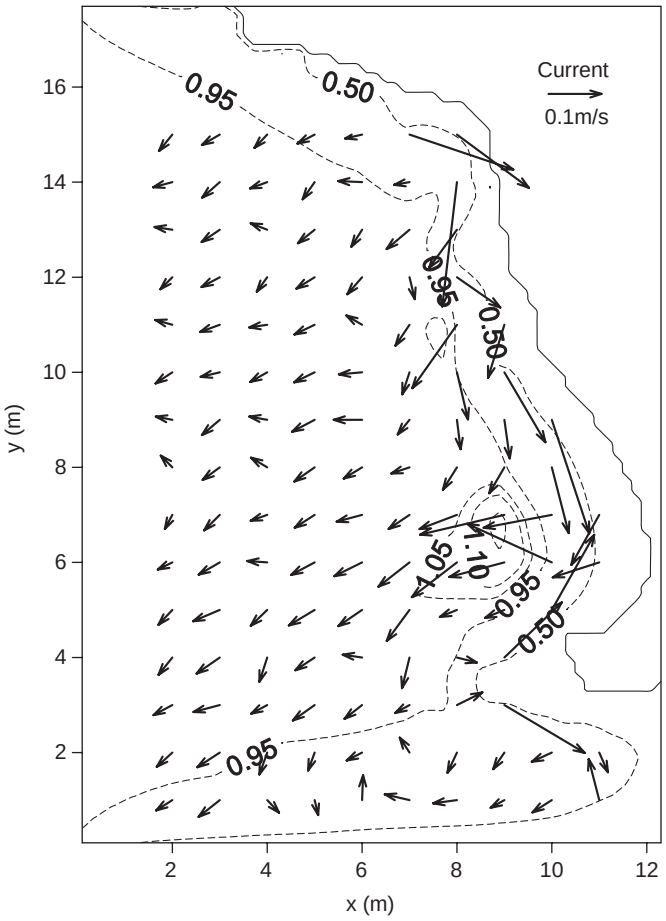

Fig. 14. Calculated wave field for uni-directional waves with currents (using Battjes and Janssen's formulation).

The along-shore and cross-shore grid cell sizes were 0.2 m × 0.2 m in the numerical model. The input wave spectrum was divided into 10 frequency bins and 36 direction bins. The current field input in each grid cell was interpolated from the measured data. The variation of water level due to wave setup was not considered in these simulations.

Figs. 10–14 show heights of the 100-year's return period incident uni-directional waves calculated with different energy dissipation formulas with or without the input current field. These results show that the wave height estimates without the input current field are quite different from the experimental data. The wave convergence in front of the concave shoreline is apparent. In contrast, the wave height estimates with the input current field were comparatively better. This clearly indicates the importance of the need to consider simulating wave–current interactions in the wave height estimates. The comparison of wave estimates for different parametric breaking formulas obtained with the effect of current in Chawla and Kirby's formula was unable to produce the extent or the intensity of wave convergence that was observed in the laboratory and prototype settings.

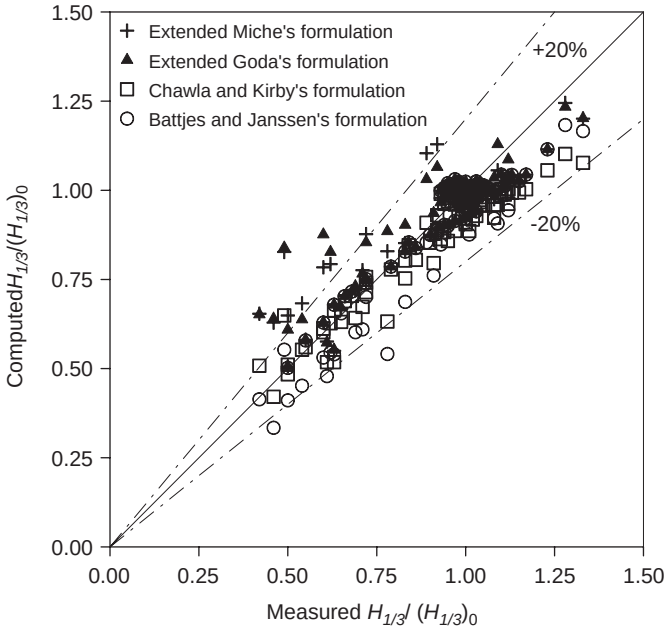

Fig. 15. Comparison between measured and calculated normalized wave heights.

Normalized significant wave height estimates with different parametric energy dissipation formulas are compared to data in Fig. 15. The percentage differences between the calculated and measured wave heights are generally less than 20 percent. The extended Miche's and extended Goda's formulas overestimated the wave height for measured normalized wave height less than 0.75. In contrast, the Battjes and Janssen's formula slightly underpredicted the wave height. Fig. 16 shows the example of calculated and measured normalized significant wave heights along longitudinal and transverse transects at $x = 9.0$ m and $y = 6.0$ m. In the simulation without current, the Battjes and Janssen's formula was used to calculate the dissipation. Calculated results with the current effects show a better agreement with data in the area of strong wave convergence, which was assumed to be caused by the opposing nearshore current.

The mean value of absolute relative error for the normalized significant wave height and the correlation coefficient between predicted and measured normalized wave heights are shown in Table 4. The sample size M in this case is 635. The two statistics calculated for different energy dissipation formulations indicate that the mean error (MAERH) in wave height prediction is less than 10 percent and the correlation coefficient is approximately 0.8. The extended Goda's and the Battjes and Janssen's formulas produced reasonably good estimates. Chawla and Kirby's formula with lower limits ($\gamma = 0.6$) predicted larger wave heights in the offshore for uni-directional waves, and performed rather poorly for multi-directional waves. For all four wave breaking formulas, the model results agree better with data for incident uni-directional waves than for multi-directional waves. Our modification of Chawla and Kirby's formula by changing γ from 0.6 to 1.0 overestimated wave heights in the shallow water where measured normalized wave height were less than 0.75. For the wave conditions simulated in this application, the modified Chawla and Kirby formula, either with the breaker criterion or breaker percentage, performed better than the original formula, producing

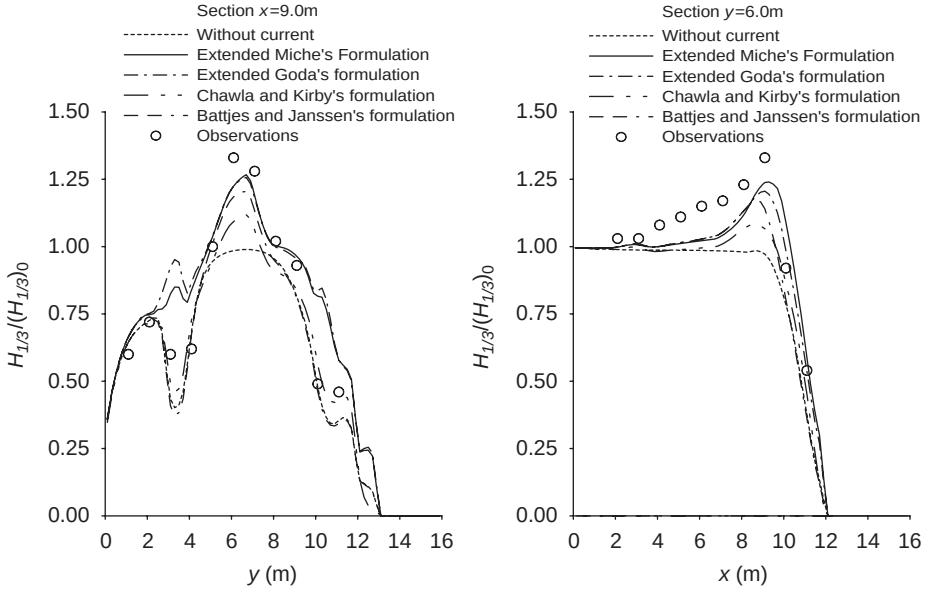

Fig. 16. Normalized wave height comparisons along longitudinal and transverse transects; simulations without current based on Battjes and Janssen's formulation: (a) longitudinal transect and (b) transverse transect.

Table 4
Statistical mean errors and correlation coefficients for complicated bathymetric coast case

	Uni-directional waves		Multi-directional waves	
	MAERH (%)	Correlation coefficient	MAERH (%)	Correlation coefficient
Extended Miche's formulation	6.55	0.83	7.44	0.79
Extended Goda's formulation	5.74	0.87	5.92	0.87
Chawla and Kirby's formulation ($\gamma = 0.6$)	6.45	0.83	7.33	0.81
Chawla and Kirby's formulation ($\gamma = 1.0$)	6.96	0.79	7.68	0.78
Chawla and Kirby 's formulation ($\gamma = 0.6$ add breaker criterion)	5.79	0.87	5.96	0.87
Chawla and Kirby's formulation ($\gamma = 0.6$ add breaker percentage)	5.48	0.88	6.09	0.88
Battjes and Janssen's formulation	5.71	0.88	6.12	0.88

similar wave height estimates as those obtained with the extended Goda's and Battjes and Janssen's formulas.

4. Concluding remarks

The suitability of four different parameterized wave breaking formulas is examined in this paper for implementation in a coastal wave transformation model. These formulas were evaluated in a phase-averaged spectral model WABED that incorporates the effects of wave diffraction, reflection, and wave–current interaction. Two data sets obtained from laboratory physical model experiments were used to evaluate appropriateness of these formulas in practical applications of WABED model. The first data set was from an experimental study for an idealized inlet, and a test condition representing a slack tide state with two steady-state ebb currents. The second experimental study investigated random wave transformation over a complex bathymetry, over which wave breaking occurred, generating strong wave-induced nearshore currents.

Performance of these parameterized wave breaking and dissipation formulas is investigated through extensive testing, and results are provided for a wide range of wave and current conditions. Statistics of the predicted wave height and measured data comparison shown in Tables 2 and 4 revealed that the extended Goda's and the Battjes and Janssen's breaking formulas consistently produced reliable and accurate wave height estimates as compared to other formulas. Therefore, these formulas are suitable for representation of wave breaking and dissipation in coastal spectral wave transformation numerical models developed for coastal inlets, structures, and navigation projects.

Acknowledgments

The first author acknowledges his appreciation to the China Scholarship Council and the Ministry of Education, Culture, Sports, Science and Technology, Japan, for their support during his stay as a visiting scholar in Disaster Prevention Research Institute, Kyoto University, Japan. Partial support for this work was received from the Key Project of Chinese Ministry of Education (no. 108065). We would like to acknowledge support for this research from Dr. Nicholas C. Kraus, Program Manager of the Coastal Inlets Research Program at the US Army Engineer R&D Center, Coastal and Hydraulics Laboratory, Vicksburg, MS, USA. Permission to publish this paper has been granted by the Headquarters, US Army Corps of Engineers.

References

Battjes, J.A., 1972. Set-up due to irregular waves. In: Proceedings of the 13th Conference on Coastal Engineering, ASCE, Vancouver, Canada, vol. 3, pp. 1993–2004.

Battjes, J.A., Janssen, J.P.F.M., 1978. Energy loss and set-up due to breaking of random waves. In: Proceedings of the 16th Conference on Coastal Engineering, ASCE, Hamburg, Germany, vol. 1, pp. 569–587.

Benoit, M., Marcos, F., Becq, F., 1996. Development of a third generation shallow-water wave model with unstructured spatial meshing. In: Proceedings of the 25th Conference on Coastal Engineering, ASCE, Orlando, USA, vol. 1, pp. 551–574.

Booij, N., Ris, R.C., Holthuijsen, L.H., 1999. A third-generation wave model for coastal regions. 1. Model description and validation. Journal of Geophysical Research 104 (C4), 7649–7666.

Bretherton, F.P., Garrett, C.J.R., 1968. Wave trains in inhomogeneous moving media. Proceeding of Royal Society, London, Series A 302, 529–554.

Briggs, M.J., Liu, P.L.-F., 1993. Experimental study on monochromatic wave–ebb current interaction. In: Proceedings of the Second International Symposium of Ocean Wave Measurement and Analysis, Waves '93, ASCE, New Orleans, USA, pp. 474–488.

Chawla, A., Kirby, J.T., 2002. Monochromatic and random wave breaking at blocking points. Journal of Geophysical Research 107 (C7), doi:10.1029/2001JC001042.

Chen, W., Panchang, V.G., Demirbilek, Z., 2005. On the modeling of wave–current interaction using the elliptic mild-slope wave equation. Ocean Engineering 32 (17–18), 2135–2164.

Dean, R.G., 1977. Equilibrium beach profiles: US Atlantic and Gulf Coasts. Ocean Engineering Technical Report No. 12, Department of Civil Engineering and College of Marine Studies, University of Delaware, Newark. DE, USA.

Goda, Y., 1970. A synthesis of breaker indices. Transaction of Japan Society of Civil Engineering 13, 227–230 (in Japanese).

Hedges, T.S., Anastasiou, K., Gabriel, D., 1985. Interaction of random waves and currents. Journal of Waterway, Port, Coastal and Ocean Engineering 111 (2), 275–288.

Iwagaki, Y., Asano, T., Yamanaka, Y., Nagai, F., 1980. Wave breaking due to currents. Annual Journal of Coastal Engineering, JSCE 27, 30–34 (in Japanese).

Lai, R.J., Long, S.R., Huang, N.E., 1989. Laboratory studies of wave-current interaction: kinematics of the strong interaction. Journal of Geophysical Research 97 (C11), 16201–16214.

Li, Y., Dong, G., 1993. Breaking of irregular waves with opposing current. Marine Science Bulletin 12 (5), 1–8 (in Chinese).

Lin, L., Demirbilek, Z., 2005. Evaluation of two numerical wave models with inlet physical model. Journal of Waterway, Port, Coastal and Ocean Engineering 131 (4), 149–161.

Lin, L., Mase, H., Yamada, F., Demirbilek, Z., 2006. Wave-action balance diffraction (CMS-Wave) model, Part 1: tests of wave diffraction and reflection at inlets. Coastal Inlets Research Program, Technical Note CIRP-TN-III-73. US Army Engineer Research and Development Center, Vicksburg, MS, USA.

Lin, L., Demirbilek, Z., Mase, H., Zheng, J., Yamada, F., 2008. CMS-wave: a nearshore spectral wave processes model for coastal inlets and navigation projects. Coastal Inlets Research Program, Coastal and Hydraulics Laboratory Technical Report ERDC/CHL-TR-08-xx. US Army Engineer Research and Development Center, Vicksburg, MS, USA.

Madsen, P.A., Sorensen, O.R., 1992. A new form of the Boussinesq equations with improved linear dispersion characteristics. Part 2: a slowly-varying bathymetry. Costal Engineering 18, 183–205.

Mase, H., 2001. Multidirectional random wave transformation model based on energy balance equation. Coastal Engineering Journal 43 (4), 317–337.

Mase, H., Kitano, T., 2000. Spectrum-based prediction model for random wave transformation over arbitrary bottom topography. Coastal Engineering Journal 42 (1), 111–151.

Mase, H., Amamori, H., Takayama, T., 2005a. Wave prediction model in wave–current coexisting field. In: Proceedings of the 12th Canadian Coastal Conference (CD-Rom), Dartmouth, Nova Scotia, Canada.

Mase, H., Oki, K., Hedges, T.S., Li, H.J., 2005b. Extended energy-balance-equation wave model for multidirectional random wave transformation. Ocean Engineering 32 (8–9), 961–985.

Miche, A., 1944. Mouvements ondulatoire de la mer en profondeur croissante ou decroissante. forme limite de la houle lors de son deferlement. application aux digues maritimes. troisieme partie. forme et proprietes des houles limites lors

du deferlement. croissance des vitesses vers la rive. Annales des ponts et chaussees, Tome 114, 369–406.
Mitsuyasu, H., 1970. On the growth of spectrum of wind-generated waves (2)—spectral shape of wind waves at finite fetch. Annual Journal of Coastal Engineering, JSCE 17, 1–7 (in Japanese).
Nwogu, O., 1993. A alternative form of the Boussinesq equations for nearshore wave propagation. Journal of Waterway, Port, Coastal and Ocean Engineering 119 (6), 618–638.
Nwogu, O., Demirbilek, Z., 2001. BOUSS-2D: A Boussinesq wave model for coastal regions and harbors. Coastal and Hydraulics Laboratory Technical Report ERDC/CHL TR-01-25. US Army Engineer Research and Development Center, Vicksburg, MS, USA.
Ostendorf, D.W., Madsen, O.S., 1979. An analysis of longshore currents and associated sediment transport in the surf zone. Report no. MITSG 79-13, MIT, p. 169.
Peregrine, D.H., 1967. Long waves on a beach. Journal of Fluid Mechanics 27 (4), 815–827.
Ris, R.C., Holthuijsen, L.H., 1996. Spectral modeling of current induced wave-blocking. In: Proceedings of the 25th Conference on Coastal Engineering, ASCE, Orlando, FL, USA, vol. 2, pp. 1247–1254.
Rivero, F.J., Arcilla, A.S., Carci, E., 1997. An analysis of diffraction in spectral wave models. In: Proceedings of the Third International Symposium of Ocean Wave Measurement and Analysis, ASCE, Reston, VA, USA, pp. 431–445.
Sakai, S., Hirayama, K., Saeki, H., 1988. A new parameter for wave breaking with opposing current on sloping sea bed. In: Proceedings of the 21st Conference on Coastal Engineering, ASCE, Costa del Sol-Malaga, Spain, vol. 2, pp. 1035–1044.
Smith, J.M., 2001. Breaking in a spectral wave model. In: Proceedings of the Fourth International Symposium of Ocean Wave Measurement and Analysis, Waves 01, ASCE, San Francisco, CA, USA, pp. 1022–1031.
Smith, J.M., Seabergh, W.C., Harkins, G.S., Briggs, M.J., 1998. Wave breaking on a current at an idealized inlet. Report CHL-98-31, US Army Corps of Engineers, Vicksburg, MS, USA.
Smith, J.M., Resio, D.T., Zundel, A.K., 1999. STWAVE: Steady state spectral wave model. Instruction Report CHL-99-1, US Army Engineer Waterways Experiment Station, Vicksburg, MS, USA.
Takayama, T., Ikeda, N., Hiraishi, T., 1991. Wave transformation calculation considering wave breaking and reflection. Report of Port and Harbor Research Institute 30 (1), 21–67 (in Japanese).
Thornton, E.B., Guza, R.T., 1983. Transformation of wave height distribution. Journal of Geophysical Research 88 (C10), 5925–5938.
Yu, Y.Y., 1952. Breaking of waves by opposing current. Transaction of American Geophysical Union 33 (1), 39–41.
Zhao, L., Panchang, V.G., Chen, W., Demirbilek, Z., Chhabbra, N., 2001. Simulation of breaking effects in a two-dimensional harbor wave prediction model. Coastal Engineering 42 (4), 359–373.
Zubier, K., Panchang, V.G., Demirbilek, Z., 2003. Simulation of waves at Duck (North Carolina) using two numerical models. Coastal Engineering Journal 45 (3), 439–469.